J Mol Model (2012) 18:4699–4708
DOI 10.1007/s00894-012-1466-4

ORIGINAL PAPER

Does the copolymer poly(vinylidene cyanide–tricyanoethylene) possess piezoelectricity?

Zhi-Yin Wang · Ke-He Su · Qiong Xu

Received: 8 November 2011 / Accepted: 13 May 2012 / Published online: 2 June 2012

Abstract The geometry, energy, internal rotation barrier, dipole moment, and molecular polarizability of the α- and β-chain models of poly(vinylidene cyanide–tricyanoethylene) [P(VDCN-TrCN)] were studied with density functional theory at the B3PW91/6-31G(d) level. The effects of the chain length and the TrCN content on the copolymer chain stability, the chain conformation, and the electrical properties of P(VDCN-TrCN) were examined and compared with those of poly(vinylidene fluoride–trifluoroethylene) and PVDCN to gauge whether P(VDCN-TrCN) would be expected to possess substantial piezoelectricity. The results of this study showed that the stability of the β conformation increases and the energy difference per monomer unit between the β- and α-chains decreases with increasing TrCN. However, introducing TrCN into VDCN will not significantly enhance the radius of curvature of the P(VDCN-TrCN) chains. The average dipole moment per monomer unit in the β-chain is affected by the chain curvature and the TrCN content. The amount of piezoelectricity present in P(VDCN-TrCN) is slightly smaller than that in PVDCN, and is less than that in poly(vinylidene fluoride–trifluoroethylene).

Z.-Y. Wang (✉) · Q. Xu
School of Chemical and Environmental Sciences,
Shaanxi University of Technology,
Hanzhong, Shaanxi 723001, People's Republic of China
e-mail: wangzy525@yahoo.com.cn

Q. Xu
e-mail: xuq@snut.edu.cn

K.-H. Su
School of Natural and Applied Sciences,
Northwestern Polytechnical University,
Xi'an, Shaanxi 710072, People's Republic of China
e-mail: sukehe@nwpu.edu.cn

Keywords Polymer physical chemistry · Ab initio calculations · Piezoelectricity · Electronic structure · Structure–property relations

Introduction

The development of new ferroelectric, piezoelectric, and magnetostrictive materials with high strain, high elastic density, and high electromechanical coupling has been a scientific and technological challenge pursued by a number of researchers in recent years. This is because ferroelectric polymeric materials offer many unique features, such as the ability to cope with high levels of strain without exhibiting structural fatigue, light weight, low cost, great mechanical strength, easy processability into thin and flexible films of various shapes and sizes, chemical inertness, substantial piezoelectric and pyroelectric properties, and—most importantly—flexible design of the molecular architecture via molecular tailoring [1–5]. The discovery of the enhanced piezoelectric activity of poly(vinylidene fluoride) (PVDF) [6] led in turn to the discovery and applications of pyroelectricity [7, 8] and ferroelectrical properties [9]. Naturally, researchers extended their work in this area to explore the chemistry, physics and technologies associated with other novel ferroelectric polymers, such as PVDF-based copolymers [10–26], odd-numbered polyimides [27, 28], cyanopolymers [29], and polyurethane [30, 31]. Significant progress in this field in terms of new materials and our understanding of structure–property relationships has been reported in the last few decades.

The most well-known and widely used of the various novel ferroelectric polymers are the family based on vinylidene fluoride (VDF) copolymerized with trifluoroethylene [P(VDF-TrFE)] [12, 19–22] or tetrafluoroethylene [P(VDF-

TeFE)] [20, 23, 24]. It has shown that the strongest piezoelectrical [32] and pyroelectrical [7, 8, 33] properties occur in the polarized β phases of these copolymers. Their large polarizabilities arise from the highly ordered arrangement of intrinsically polar $-[CH_2–CF_2]-$ monomers, where each VDF monomer has a nonzero dipole moment that is directed perpendicular to the carbon backbone.

Given this explanation, we would expect that it might be possible to synthesize a polymer containing monomers with large dipole moments and to align the dipoles to form a polar crystal that exhibits even stronger piezoelectricity and pyroelectricity. Since the dipole moment of the repeating unit $-[CH_2–C(CN)_2]-$ is 4.0~4.5 Debye [34, 35] in the *trans* conformation (which is much higher than the value of 1.96 Debye [25] in VDF), it is possible to achieve a large piezoelectric constant. Therefore, polymers or copolymers containing C-C≡N groups, such as poly(vinylidene cyanide) (PVDCN) [36, 37], polyacrylonitrile (PAN) [38–40], poly (vinylidenecyanide vinylacetate) (PVDCN/VAc) [41–44], and polyphenylethernitrile (PPEN) [36, 45], have received much attention in the study of electromechanical transducers, nonvolatile memories, and in the field of biomedicine, which also benefits from their unique features of low density and low acoustic impedance (close to the levels exhibited by water and solutions in the human body).

Vinylidene cyanide (VDCN) is known to polymerize with a wide variety of co-monomers [such as vinylacetate (VAc), styrene and dienes] to form alternating copolymers [36, 46, 47]. Among those, the most promising material is the copolymer poly(vinylidenecyanide–vinylacetate) P(VDCN/VAc), which has very special features [34, 48–50]: it is a perfectly alternating copolymer [36] and an amorphous polymer with a high glass-transition temperature [47], and it possesses strong piezoelectric activity [42, 43, 51], a high dielectric relaxation strength [41, 48], and a large enthalpy of relaxation. When P(VDCN-VAc) was investigated using NMR [42, 44, 50], the results indicated that a combination of several factors associated with the microstructure and conformation may be responsible for its piezoelectricity. The piezoelectricity (d_{31}) of drawn and poled films of P(VDCN/VAc) is comparable to that of PVDF in the temperature range 20–100 °C [43]. In particular, this copolymer shows a very large dielectric relaxation strength that reaches as high as 125 [41, 48], which is one of the largest values seen in polymers. Miyata and coworkers [34, 43] also reported an electromechanical coupling factor of 0.25 for this copolymer, which is greater than that of PVDF. Such high activity suggests that considerably remanent polarization is created during poling.

Copolymerization of different monomers or the blending of different types of polymers is an important way of improving the material properties of a polymer. The copolymerization of different monomers makes it possible to synthesize a series of highly crystalline ferroelectric copolymers such as P(VDF-TrFE) and P(VDF-TeFE). Xiao et al. [52] reported that highly ordered polymethylvinylidenecyanide [PMVC, $-(CH(CH_3)\text{-}C(CN)_2)_n-$] can be realized if the films are prepared by the Langmuir–Blodgett (LB) technique. Analyses of the electronic structures of P(VDF-TrFE, 70:30) and PMVC show that they are in the all-*trans* configuration, with all of the dipoles aligned. PVDF and its copolymers P(VDF-TrFE) and P(VDF-TeFE) [10–26] as well as the copolymers of VDCN with vinyl acetate (VAc), vinyl benzoate (VBz), vinyl pivarate (VPiv), and vinyl isopropionate (VPr) [36, 46, 47] have been investigated in detail. However, P(VDCN-TrCN), which may be regarded as homologous to P(VDF-TrFE) if all of the fluorine atoms are substituted for nitrile groups, has not been investigated either experimentally or theoretically. It is interesting to note that introducing TrFE monomer units into VDF greatly enhances the crystalline and ferroelectric properties of the copolymer P(VDF-TrFE) [1, 53–56]. For example, P(VDF-TrFE) was found to display a much greater degree of crystallinity (up to 90 %) than PVDF, yielding a higher remanent polarization, a lower coercive field, and much sharper hysteresis loops. TrFE also extends the working temperature of the copolymer by about twenty degrees (up to about 100 °C) [57]. Another attractive feature is that the co-monomers force the copolymer chain to form an all-*trans* conformation. Consequently, we hope that the crystallinity, piezoelectricity, and pyroelectricity are improved by introducing TrCN into VDCN to form the P(VDCN-TrCN) copolymer.

Since the orientation polarization of molecular dipoles is responsible for the piezoelectricity in amorphous polymers, the molecular structure of the polymer must be considered to be one of the most important influences on piezoelectric activity. The chain conformation and structure are especially important for understanding the origin of piezoelectricity in not only crystalline but also amorphous polymers. Encouraged by previous work reported in the literature on the structure–property relationships for PVDF [25], P(VDF-TrFE) [26], P(VDF-TeFE) [18], PVDCN [37], P(VDCN-TrFE) [58], P(VDCN-TeFE) [59], and P(VDCN-TeCN) [60], which were studied using density functional theory, this work carried out theoretical calculations relating to the internal rotation potentials, geometries, and electrical properties of α- and β-chain P(VDCN-TrCN) using a first-principles DFT and a number of structural models. The energies, permanent dipole moments, and molecular polarizabilities of the models were obtained. The effects of chain length and content of TrCN on the electrical properties of α- and β-chain P(VDCN-TrCN) were predicted and compared with those of PVDCN, P(VDF-TrFE), and P(VDCN-TrCN).

Computational details

DFT at the B3PW91/6-31G(d) [61, 62] level was employed, using the GAUSSIAN-09 software package [63]. This level of theory is the same as that used in the study of PVDF [25], P(VDF-TrFE) [26], P(VDF-TeFE) [18], PVDCN [37], P(VDCN-TrFE) [58], P(VDCN-TeFE) [59], and P(VDCN-TeCN) [60], thus facilitating comparisons. The internal rotation potentials (IRP) were calculated using the dimer models $H(CH_2C(CN)_2)$–$CH(CN)C(CN)_2)H$ and $H(C(CN)_2CH_2$–$C(CN)_2CH(CN))H$. The geometries of α- and β-chain P(VDCN-TrCN) with different chain lengths (n) and TrCN contents were optimized, and the molecular energies and dipole moment vectors (μ_x, μ_y, μ_z) were then obtained. The chain models were $H[(CH_2C(CN)_2)$–$(CH(CN)C(CN)_2)]_mH$ ($n=2m$), $H[(CH_2C(CN)_2)_2$–$(CH(CN)C(CN)_2)]_mH$, ($n=3m$), and $H[(CH_2C(CN)_2)_3$–$(CH(CN)C(CN)_2)]_mH$ ($n=4m$) for different TrCN contents. Those models correspond to the ideal arrangement of the alternating copolymer based on the features of the copolymer [36, 46–48, 64]. The exact molecular polarizability tensors α_{xx}^{mol}, α_{xy}^{mol}, α_{yy}^{mol}, α_{xz}^{mol}, α_{yz}^{mol} and α_{zz}^{mol} were obtained using frequency analyses. Each tensor (e.g., α_{xy}^{mol}) is defined as the linear response to an externally applied electric field [65] ($\mu_x^{ind}=\alpha_{xy}^{mol}E_y^{ext}$, where μ^{ind} is the induced molecular dipole moment, E^{ext} is the magnitude of the applied electric field, and *x, y, z* represent the Cartesian components).

Results and discussion

Internal rotation of related dimers

It is well known that the chain conformation depends mainly on the polymer chain packing, the electrostatic repulsion of internal dipoles, and the effect of steric hindrance. Therefore, the rotation of a monomer unit in a polymer chain is much more complex than that in a dimer model. However, IRP is the most important intrinsic property that reflects the conformation distribution of a polymer chain. Therefore, for computational convenience, the dimer model of the P(VDCN-TrCN) chain was examined to emphasize the intramolecular rotation potentials.

Similar to the copolymers P(VDF-TrFE) [26] and P(VDCN-TrFE) [58], two dimer models for the chain of P(VDCN-TrCN), $H[CH_2C(CN)_2$–$CH(CN)C(CN)_2]H$ (referred to as model I) and $H[C(CN)_2CH_2$–$C(CN)_2CH(CN)]H$ (referred to as model II), were drawn. The rotation angle starts and terminates at the C–C–C–C *eclipsed* conformation (corresponding to a C–C–C–C dihedral angle of both zero and 360°). Newman projections of the *eclipsed*, *gauche*, and *trans* configurations for the P(VDCN-TrCN) dimer models are shown in the upper panel of Fig. 1, while IRP curves are shown in the lower panel (model I is donoted by solid circles, and model II by half-solid circles). Also plotted in the lower panel are the curves for P(VDF-TrFE) from [27] (solid triangles for the model I, $H[CH_2CF_2$–$CHFCF_2]H$, and half-solid triangles for model II, $H[CF_2CH_2$–$CF_2CHF]H$), while the curve for the only dimer model of PVDCN, as taken from [37], is depicted by star symbols. The potential energies of the most stable conformations of P(VDCN-TrCN) [curve (a) at 280° and curve (b) at 78°], $P(VDF\text{-}TrFE)_I$ [curve (c) at 290°], and $P(VDF\text{-}TrFE)_{II}$ [curve (d) at 295°] [26] are plotted in the lower panel of Fig. 1, using the energy of PVDCN [curve (e) at ±47°] [37] as a reference.

In model I of P(VDCN-TrCN), the conformation of the terminal $–CH_3$ group is determined by geometry optimizations without any restriction. The terminal $–C(CN)_2H$ group is arranged to ensure that the conformation is the β-form (all-*trans*) when the C–C–C–C dihedral angle is 180°. The results show that both of the terminal groups are in a staggered conformation with respect to the nearest (directly bonded) $–C(CN)_2$ and –CH(CN) segments. Similar to P(VDF-TrFE), these segments differ between the two P(VDCN-TrCN) dimers, and curves (a) and (b) are also not symmetric, which contrasts with the symmetric curves seen for PVDCN [37] and PVDF [25]. This means that the α-form (i.e., *tgtg′*, where *g* refers to *gauche* and *t* refers to *trans*, and the prime symbol on *g′* indicates that the dihedral angle is opposite to that for the *g* conformation with respect to the reference plane *t*) has different conformational angles in the *tg* and *tg′* models. The value for the *g* conformation is 46°, and that for *g′* is −80° (or 280°) in model I. These values are 78° and −53° (or 307°) in model II. The respective angles are 53° (for *g*) and 290° (for *g′*) in $P(VDF\text{-}TrFE)_I$, 53° (for *g*) and 295° (for *g′*) in $P(VDF\text{-}TrFE)_{II}$ [26], ±47° in PVDCN [37], and ±55° in PVDF [25]. Therefore, the angle in $P(VDCN\text{-}TrCN)_I$ is 1° smaller (for *g*) and 33° (for *g′*) larger than that in PVDCN [37]. The same angle in $P(VDCN\text{-}TrCN)_{II}$ is 31° (for *g*) larger and 6° (for *g′*) smaller than that in PVDCN. Conformational differences between models I and II and among the different systems are also shown in Fig. 1. It is apparent that the most stable β conformation of P(VDCN-TrCN) will be a slightly distorted all-*trans* plane with a dihedral angle of 166° for model I and 162° for model II. These angles are close to that (164°) seen in PVDCN. Additionally, the "ideal β-chain conformation" (i.e., all-*trans ttt*) of P(VDCN-TrCN) in model I or model II is no longer (compared with PVDCN) a transition state, as shown in the inset plot of the lower panel of Fig. 1.

For the dimer model I of P(VDCN-TrCN), it is clear that the *tg′* conformation is more stable than *tg* by 1.9 kJ mol^{-1}, but the *tg* conformation is more stable than *tg′* by 15.7 kJ mol^{-1} for the dimer model II of P(VDCN-TrCN). The energy differences, $E_\beta - E_{\alpha(g)}$ and $E_\beta - E_{\alpha(g')}$, between the β and the α conformations are 0.5 and 2.4 kJ mol^{-1},

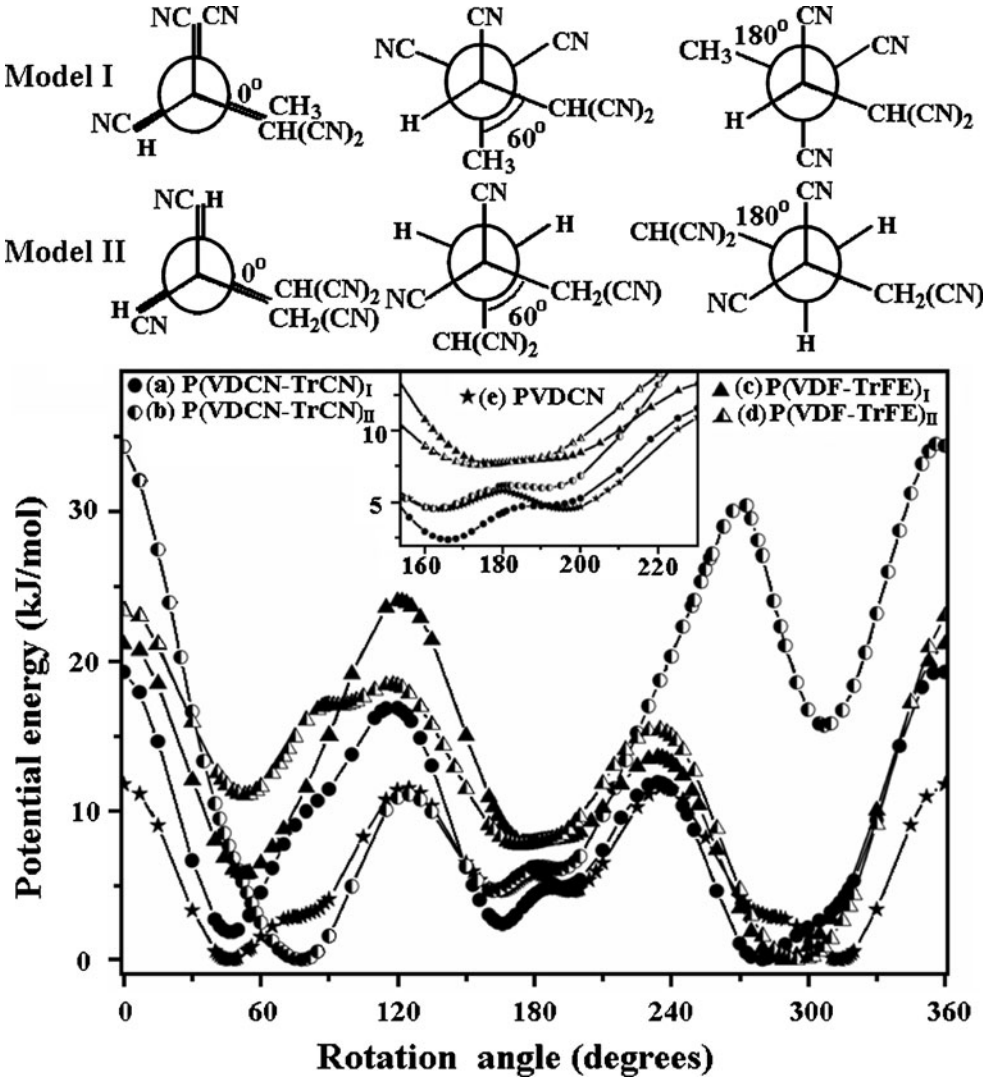

Fig. 1 Newman projections of the *eclipsed*, *gauche*, and *trans* configurations of dimer models I and II for P(VDCN-TrCN; *left*, *middle*, and *right* in *upper panel*), and a comparison of the internal rotation potential energy curves obtained from B3PW91/6-31G(d) calculations (*lower panel*): curves (*a*) and (*b*) are for the models H[($CH_2C(CN)_2$)–(CH(CN)$C(CN)_2$)]H (model I) and H[$C(CN)_2CH_2$–$C(CN)_2$CH(CN)]H (model II) of the chain of the copolymer P(VDCN-TrCN), curves (*c*) and (*d*) are for the models H((CH_2CF_2)–($CHFCF_2$))H (model I) and H((CF_2CH_2)–(CF_2CHF))H (model II) of the chain of the copolymer P(VDF-TrFE) [26], while curve (*e*) is for the dimer model H(($CH_2C(CN)_2$))$_2$H of PVDCN [37]

respectively, for model I. These values are 4.6 kJ mol^{-1} and −11.1 kJ mol^{-1} for model II. All of them are smaller than the value in PVDCN (5.9 kJ mol^{-1}), which suggests that the β conformation of the P(VDCN-TrCN) copolymer will be more stable than PVDCN [37]. The fact that the β conformation of P(VDCN-TrCN) is more stable than the α conformation thermodynamically is a useful property for the material of interest. The energy barriers are 14.5 kJ mol^{-1} and 9.5 kJ mol^{-1} for the β→α(*g*) and β→α(*g*′) transitions in model I, and 6.4 kJ mol^{-1} and 20.5 kJ mol^{-1} for those transitions in model II, respectively. It is interesting that both values in model I and the latter in model II (14.5, 9.5, and 20.5 kJ mol^{-1}) are larger than 6.9 kJ mol^{-1}, which is the barrier in PVDCN [37], while the former value for model II (6.4 kJ mol^{-1}) is very close to that. Therefore, the β→α transition in P(VDCN-TrCN) should be more difficult to realize than that in PVDCN once it is formed. This is also a very useful property that can be used in practical applications to prevent the piezoelectric phase from depolarizing. The energy barriers for the α(*g*)→β and α(*g*′)→β transitions are 15.0 kJ mol^{-1} and 11.9 kJ mol^{-1} in model I and 11.0 kJ mol^{-1} and 25.8 kJ mol^{-1} in model II, respectively. These values are comparable with the 11.5 kJ mol^{-1} seen in PVDCN [37] and the 16.3 kJ mol^{-1} seen in PVDF [25], except for α(*g*′)→β transitions in model II. That implies that it will be feasible (or slightly more difficult) to prepare the polarized phase in the copolymer P(VDCN-TrCN).

Structure and stability

In practice, piezoelectric polymer materials are usually grown on substrates. The interaction between the polymer chain and the substrate, and the intramolecular stress existing in the polymer chain are important that will influence the ordered align of the polymer chains on the substrate. Therefore, information on the structure, stability, and curvature of the chain will aid our understanding of these interactions. In order to explore the structure and stability of P(VDCN-

TrCN) with different TrCN contents, the structures of copolymers with alternate α- (*tgtg′*) and β- (*ttt*) chains with lengths of 2 to *n* monomers (*n*=2 to 10 or 14) in the models $H[(CH_2C(CN)_2)–(CH(CN)C(CN)_2)]_mH$ (*n*=2*m*), $H[(CH_2C(CN)_2)_2–(CH(CN)C(CN)_2)]_mH$ (*n*=3*m*) and $H[(CH_2C(CN)_2)_3–(CH(CN)C(CN)_2)]_mH$ (*n*=4*m*) were optimized and compared with those of PVDCN [37], P(VDCN-TrFE) [58], and P(VDF-TrFE) [26]. The mole fractions of TrCN in P(VDCN-TrCN) were 0.50, 0.33, and 0.25. The β-chains were designed to comply with the ideal conformation (i.e., the dihedral angle for all of the backbone carbons was fixed at 180°) in all of the models examined in this work. The third –CN group of TrCN (–CH(**CN**)–$C(CN)_2$–) in P(VDCN-TrCN) was arranged alternately with respect to the chain axis to simulate the most probable orientation of TrCN in the polymerization reactions.

The structures optimized with B3PW91/6-31G(d) for the 9-, 12-, and 14-monomer unit models are shown in Fig. 2. Figures 2a–b are the β- and α-chains of P(VDCN-TrCN) with 14 monomers and a mole fraction of TrCN in $H[(CH_2C(CN)_2)–(CH(CN)C(CN)_2)]_7H$ of 0.5. Figures 2c–d are the β- and α-chains with nine monomers and a mole fraction of TrCN in $H[(CH_2C(CN)_2)_2–(CH(CN)C(CN)_2)]_3H$ of 0.33. Figures 2e–f are the β- and α-chains with 12 monomers and a mole fraction of TrCN in $H[(CH_2C(CN)_2)_3–(CH(CN)C(CN)_2)]_3H$ of 0.25. Similar to the arched α-PVDCN homopolymer [37], the α-chains of the P(VDCN-TrCN) copolymers containing TrCN at mole fractions of 0.50 and 0.25 (Fig. 2b and f) also exhibit a bent near-planar structure, but the latter has a larger radius of curvature than the former. Interestingly, the chain containing TrCN at a mole fraction of 0.33 (Fig. 2d) is nearly linear. This linear chain might favor crystal formation or show enhanced crystallinity.

Similar to the ideal β-chain structures of PVDCN [37] and P(VDF-TrFE) [26], all of the ideal β-chains in the P(VDCN-TrCN) copolymer models were curved, mainly due to the electrostatic repulsion between the C-C≡N groups on one side of the chain backbone. It is interesting that the mean radius of curvature of the β-chain increases with increasing content of TrCN. The values are 8.93, 9.24, and 9.70 Å in P(VDCN-TrCN) with mole fractions of TrCN of 0.25, 0.33, and 0.50, respectively. The mean radius of curvature in the alternate copolymer β−P(VDCN-TrCN) is slightly larger than that in the PVDCN homopolymer (about 8.5 Å) [37]. This is similar to the results obtained from previous calculations of the introduction of TrFE into VDCN, which was found to lead to reduced curvature of the P(VDCN-TrFE) chains because of the smaller electrostatic repulsion between the negative N and F atoms on one side of the backbone at larger distances [$R_{N–F}$≈3.1 Å in P(VDCN-TrFE)] [58]. This facilitates the directional arrangement of dipoles in the alternating copolymer [58]. However, introducing TrCN into VDCN does not significantly enhance the mean radius of curvature of the copolymer chains. This may be from the analogical chemical condition in the PVDCN and P(VDCN-TrCN) systems. Since polymer chains with low curvature (or a large radius of curvature) are easier to arrange in an orderly manner on substrates due to the smaller strain involved, the radius of curvature of the polymer chain can be regarded as a measure of the interaction between the polymer chains and the substrate if a piezoelectric film is fabricated. Therefore, similar to the PVDCN homopolymer, the bulk P(VDCN-TrCN) copolymer with relatively long chains would be difficult to align in an orderly manner (in order to enhance the amount of ferroelectricity) or to crystallize (i.e., the bulk copolymer would be difficult to prepare as a crystal phase).

Figure 3 plots the energy difference per monomer unit between the β- and the α-chains of P(VDCN-TrCN), i.e., $(E_\beta - E_\alpha)/n$ vs. chain length. Curves (a), (b), and (c) in Fig. 3

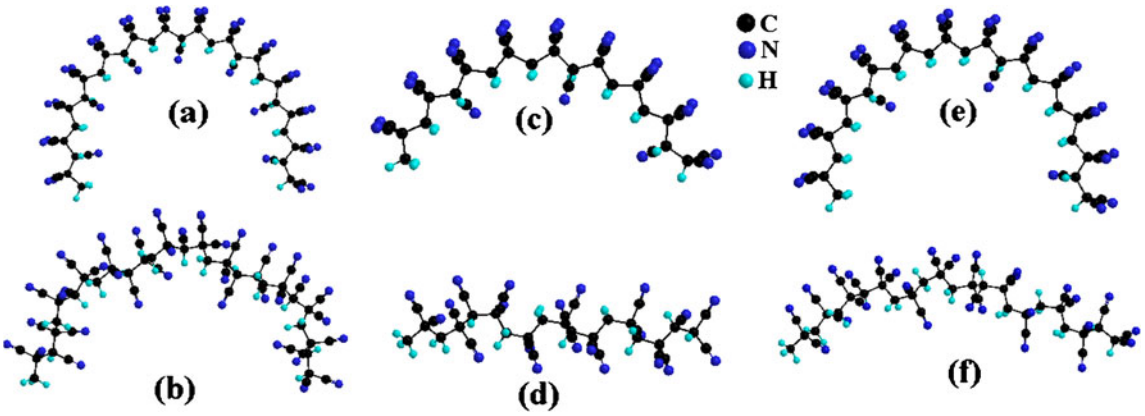

Fig. 2a–f P(VDCN-TrCN) structures optimized via B3PW91/6-31G(d) calculations: **a** and **b** refer to β- and α-chain P(VDCN-TrCN) with 14 monomers and a TrCN mole fraction of 0.5 in the $H[(CH_2C(CN)_2)–(CH(CN)C(CN)_2)]_7H$ model. **c** and **d** refer to β- and α-chain P(VDCN-TrCN) with nine monomers and a TrCN mole fraction of 0.33 in the $H[(CH_2C(CN)_2)_2–(CH(CN)C(CN)_2)]_3H$. **e** and **f** refer to β- and α-chain P(VDCN-TrCN) with 12 monomers and a TrCN mole fraction of 0.25 in the $H[(CH_2C(CN)_2)_3–(CH(CN)C(CN)_2)]_3H$ model

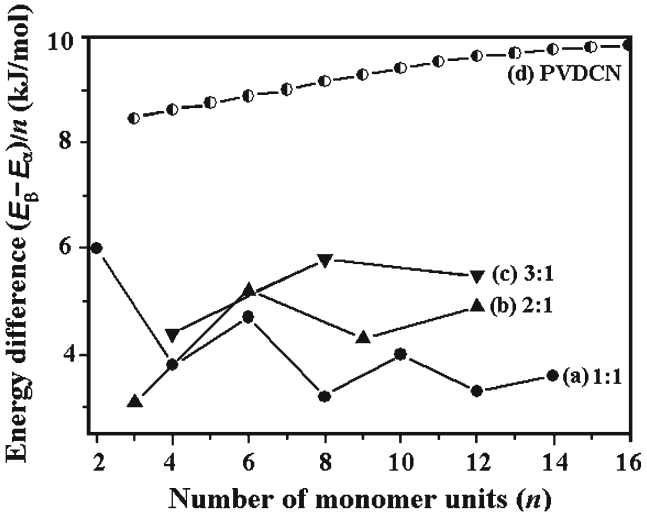

Fig. 3 Energy differences per monomer unit between the β- and α-chains: $(E_\beta - E_\alpha)/n$ vs. chain length obtained with B3PW91/6-31G(d). Curve (*a*) refers to the H[$(CH_2C(CN)_2)$–$(CH(CN)C(CN)_2)]_m$H model (n=2m) of P(VDCN-TrCN); curve (*b*) relates to the H[$(CH_2C(CN)_2)_2$–$(CH(CN)C(CN)_2)]_m$H model (n=3m) of P(VDCN-TrCN); curve (*c*) refers to the H[$(CH_2C(CN)_2)_3$-$(CH(CN)C(CN)_2)]_m$H model (n=4m) of P(VDCN-TrCN); and curve (*d*) relates to the H[$(CH_2C(CN)_2)]_n$H model of the PVDCN homopolymer from [37]

relate to copolymer chains containing 2 to n ($n \leq 14$) monomer units, and TrCN mole fractions of 0.50, 0.33, and 0.25. Curve (d) in Fig. 3 shows the energy difference for the PVDCN homopolymer [37] for comparison.

Similar to what is seen for the copolymer P(VDCN-TrFE) [58], the energy difference of each P(VDCN-TrCN) also converges with n to become almost constant, with some fairly regular oscillations (the amplitude of the energy oscillations is around ±0.5 kJ mol^{-1} in each case). For the models with different TrCN contents, represented by curves (a)–(c) in Fig. 3, the energy differences increase with decreasing TrCN content. The average values (3.5, 4.6, and 5.6 kJ mol^{-1} for (a)–(c), respectively) for the energy differences are also listed in Table 1, and they are smaller than the average value of about 9.8 kJ mol^{-1} for the PVDCN homopolymer [37]. This result shows that introducing TrCN into VDCN causes the formation of the low-energy *trans* conformation (or β-chains) to be favored. However, the energy difference (3.5 kJ mol^{-1}) for P(VDCN-TrCN) chains with a mole fraction of TrCN of 0.50 is larger than that of the P(VDCN-TrFE) chain with a mole fraction of TrFE of 0.50 (0.3 kJ mol^{-1}) [58]. This shows that the effect of the TrCN monomer on the energy difference of P(VDCN-TrCN) is not as significant as the effect of the TrFE monomer on the energy difference of P(VDCN-TrFE) [58]. In other words, if all of the F atoms in the TrFE monomer in the P(VDCN-TrFE) copolymer are substituted for –CN groups to form the P(VDCN-TrCN) copolymer, the resulting increase in the stability of the β-chains is no larger than the stability of the β-chains in the P(VDCN-TrFE) copolymer.

Dipole moment and mean polarizability

The electric response properties are of fundamental importance in an piezoelectric polymer, and are determined by its conformation, the stability of the molecular aggregate, the electric dipole, and the polarizability. In order to examine the effect of chain length and TrCN content on the electrical properties of P(VDCN-TrCN), the average permanent dipole moment per monomer unit $\mu=(\mu_x^2+\mu_y^2+\mu_z^2)^{1/2}/n$ and the mean polarizability per monomer unit $\alpha=(\alpha_{xx}+\alpha_{yy}+\alpha_{zz})/3n$ [65] were calculated for the models with different chain lengths (n units) and different TrCN contents. These results, as well as those for the β- and α-chains of PVDCN [37], are plotted in Figs. 4 and 5.

The overall contribution of a monomer unit to the dipole moment decreases with increasing chain length both for α-chain PVDCN and P(VDCN-TrCN) containing a mole fraction of TrCN of 0.50~0.25 (Fig. 4, curves a, c, e, g). However, the values do not always decrease evenly; they show some fairly regular oscillations due to the complexity of the α-chain structures. Similar to what is seen for the β-chain P(VDF-TrFE) [26] and β-chain P(VDCN-TrFE) [58] systems, the contribution to the dipole moment per monomer unit decreases with increasing chain length for all β-chain P(VDCN-TrCN) models (Fig. 4, curves d, f, h). This is also due to the fact that the dipole moment of an individual monomer unit is perpendicular to the chain, but the β-chains are curved (due to the electrostatic repulsion between the C–C≡N groups on one side of each chain), as shown by curves (a), (c), and (e) in Fig. 2. Figure 4 also shows that the contribution to the dipole moment per monomer unit decreases with increasing TrCN content in P(VDCN-TrCN). This is because the monomer –[$CH(CN)C(CN)_2$]– has a smaller dipole moment than the monomer −[$CH_2C(CN)_2$]−. The decrease in the dipole moment contribution per monomer unit with increasing chain length (n) varies with TrCN content of the β-chain P(VDCN-TrCN). The slopes of the curves decrease in the following order: homopolymer PVDCN > P(VDCN-TrCN) copolymer with a mole fraction of TrCN of 0.25 > that with a mole fraction of 0.33 > that with a mole fraction of 0.50. This is consistent with the curvatures of the β-chain P(VDCN-TrCN) models, among which the P(VDCN-TrCN) with a mole fraction of TrCN of 0.50 has the maximum radius of curvature and the minimum decrease in the dipole moment with chain length. For β-chain P(VDCN-TrCN) with 12 monomer units and a mole fraction of TrCN of 0.50, although the dipole moment contribution per monomer unit of 4.17×10^{-30} C m is higher than that of the β-chain P(VDF-TrFE) with 12 monomer units and a mole fraction of TrFE of 0.50 (dipole moment

Table 1 Energy differences per monomer unit between the α- and β-chains for P(VDCN-TrCN) copolymers with different VDCN contents, as well as the dipole moments and mean polarizabilities per monomer unit for both P(VDCN-TrCN) and PVDCN, as obtained from B3PW91/6-31G(d) calculations

	VDCN content in the copolymer (mole fraction)			
	1.00	0.75	0.67	0.50
$(E_\beta - E_\alpha)/n$ (kJ mol^{-1})	9.8[a]	5.6[b]	4.6[c]	3.5[d]
$(E_\beta - E_\alpha)/n$ (kJ mol^{-1})[e]	9.8	5.8	3.7	0.3
Contribution to the dipole moment per unit[f] (10^{-30} C m)	5.12[a]	4.65[b]	4.48[c]	4.17[d]
Mean polarizability per monomer unit (10^{-40} C m^2 V^{-1})	7.29[a]	7.79[b]	7.95[c]	8.26[d]

[a] PVDCN with the H[$(CH_2C(CN)_2)$]$_n$H model, obtained from [37]

[b] P(VDCN-TrCN) with the H[$(CH_2C(CN)_2)_3$–$(CH(CN)C(CN)_2)$]$_m$H model, n=4m

[c] P(VDCN-TrCN) with the H[$(CH_2C(CN)_2)_2$–$(CH(CN)C(CN)_2)$]$_m$H model, n=3m

[d] P(VDCN-TrCN) with the H[$(CH_2C(CN)_2)$–$(CH(CN)C(CN)_2)$]$_m$H model, n=2m

[e] The energy difference per monomer unit in P(VDCN-TrFE) for comparison, obtained from [58]

[f] β-Chain with 12 monomer units; data are from Fig. 4

contribution per monomer unit: 3.88×10^{-30} C m) [26], this value is smaller than that of the β-chain PVDCN with 12 monomer units (5.12×10^{-30} C m) [37] and the β-chain P(VDCN-TrFE) with 12 monomer units (6.32×10^{-30} C m) [58]. Typical numerical results for the P(VDCN-TrCN) chains with 12 monomer units are listed in Table 1. Compared with the PVDCN homopolymer, the dipole moment contribution per monomer unit in the P(VDCN-TrCN) copolymer is not significantly enhanced. However, if we compare the introduction of the TrFE monomer into VDCN with the introduction of the TrCN monomer into VDCN, the dipole moment contribution per monomer unit is smaller in P(VDCN-TrCN). This result suggests that the piezoelectricity of P(VDCN-TrCN) with a mole fraction of TrCN of 0.50 may be comparable with (or slightly smaller than) that of PVDCN, but it will be inferior than that of the P(VDCN-TrFE) copolymer [58]. Obviously, the poor crystallinity and the rapid decrease in the dipole moment contribution per monomer unit with increasing chain length of P(VDCN-TrCN) will cause the piezoelectricity of P(VDCN-TrCN) with a mole fraction of TrCN of 0.50 to be inferior to that of the P(VDF-TrFE) copolymer too [26].

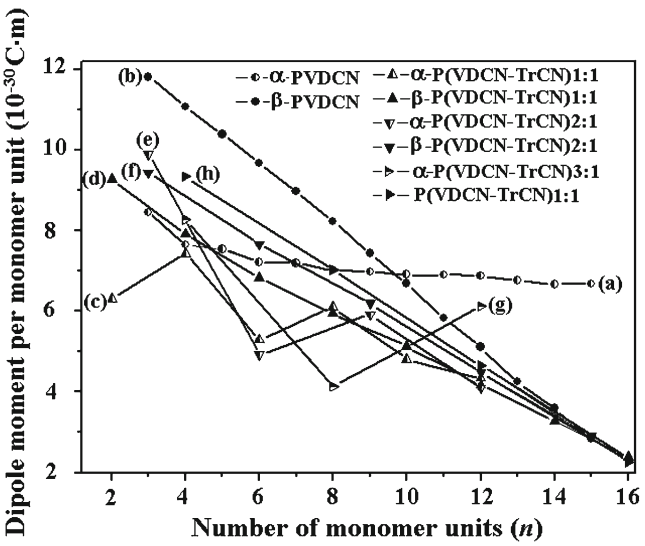

Fig. 4 Dipole moment per monomer unit vs. chain length of P(VDCN-TrCN) and PVDCN (*solid* and *half-solid symbols* indicate data for the β- and α-chains, respectively): curves (*a*) and (*b*) refer to PVDCN (data from [37]), which is included for comparison purposes; (*c*) and (*d*) refer to P(VDCN-TrCN) with a mole fraction of TrCN of 0.50; (*e*) and (*f*) refer to P(VDCN-TrCN) with a mole fraction of TrCN of 0.33; (*g*) and (*h*) refer to P(VDCN-TrCN) with a mole fraction of TrCN of 0.25

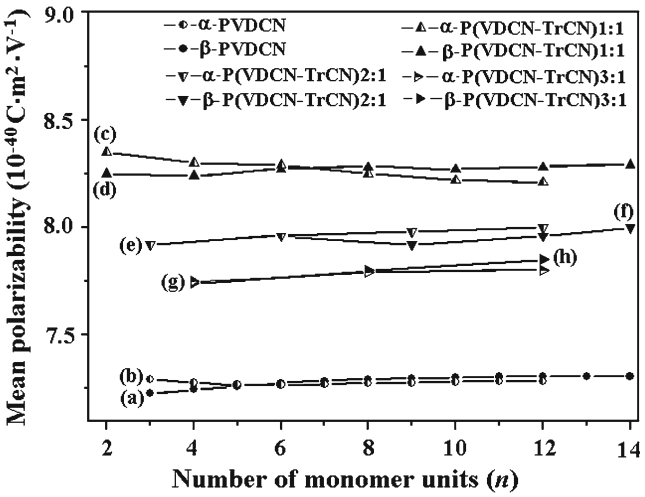

Fig. 5 Mean polarizability per monomer unit vs. the length of the copolymer chain (*solid* and *half-solid symbols* indicate data for the β- and α-chains, respectively): curves (*a*) and (*b*) refer to PVDCN (data from [37]); (*c*) and (*d*) refer to P(VDCN-TrCN) with a mole fraction of VDCN of 0.50; (*e*) and (*f*) refer to P(VDCN-TrCN) with a mole fraction of VDCN of 0.67; (*g*) and (*h*) refer to P(VDCN-TrCN) with a mole fraction of VDCN of 0.75

The contribution to the dipole moment per monomer unit in β-chain P(VDCN-TrCN) with 12 monomer units is plotted against the VDCN content in Fig. 6 (curve a). This figure shows a very weak parabolic dependence of the dipole moment per monomer on the VDCN content. This arises because the chain curvature increases slightly with increasing VDCN content (as discussed in the section "Structure and stability"), which leads to a decrease in the dipole moment contribution. This behavior is similar to that observed for the copolymers P(VDF-TrFE) [26] and P (VDCN-TrFE) [58] containing different contents of TrFE. Fitting a parabolic equation to the data allows the contribution to the dipole moment per monomer unit (in 10^{-30} C m) to be estimated for β-chain P(VDCN-TrCN) with 12 monomer units at any mole fraction x of VDCN in the range x = 0.50–1.00 (with a correlation coefficient of 0.9999). Fitting a linear equation (with a correlation coefficient of 0.9999) instead leads to the following equations of best fit:

$$\mu_{(12\text{monomers})} = 3.219 + 1.897x + 0.005x^2 \quad (1)$$

$$\mu_{(12\text{monomers})} = 3.216 + 1.904x. \quad (2)$$

Figure 5 shows that the mean polarizability per monomer unit of β-chain P(VDCN-TrCN) or PVDCN is very similar to or slightly higher than that of the corresponding α-chain. Varying the chain length does not significantly change the mean polarizability of α- or β-chain P(VDCN-TrCN) or PVDCN. However, the absolute value of the mean polarizability per monomer unit increases with increasing TrCN content in P(VDCN-TrCN). This is because the mean polarizability of the TrCN monomer, –[CH(CN)C$(CN)_2$]–, is larger than that of the VDCN monomer, –[CH_2C$(CN)_2$]–

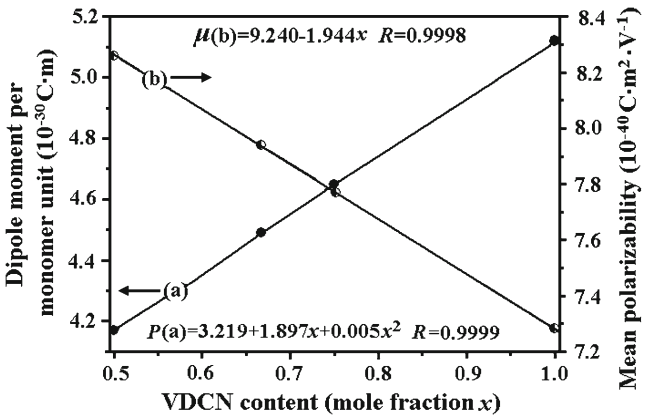

Fig. 6 Curve (*a*; left-hand axis) shows the dependence of the contribution to the dipole moment per monomer unit on VDCN content in β-chain P(VDCN-TrCN) with 12 monomer units. Curve (*b*; right-hand axis) shows the dependence of the mean polarizability per monomer unit on the VDCN content in P(VDCN-TrCN). Data are from Table 1 (see Fig. 5, curve a). These values (in 10^{-40} C m^2 V^{-1}) are 8.26, 7.95, and 7.79 (see Table 1), respectively, for alternate P(VDCN-TrCN) copolymers with mole fractions of VDCN of 0.50, 0.67, and 0.75. The values are 7.29×10^{-40} and 3.63×10^{-40} C m^2 V^{-1} for PVDCN [37] and PVDF [25], respectively.

The mean polarizabilities per monomer unit of β-chain P (VDCN-TrCN) models with different VDCN contents are plotted in Fig. 6b. Fitting an equation to this data provides an estimate of the mean polarizability per monomer unit (in 10^{-40} C m^2 V^{-1}) of P(VDCN-TrCN) for any mole fraction x of VDCN in the range 0.50~1.00. Fitting a linear equation (see below) allows fairly accurate estimates to be obtained (the correlation coefficient is 0.9998):

$$P = 9.240 - 1.944x. \quad (3)$$

Conclusions

DFT-B3PW91/6-31G(d) has been employed to investigate the internal rotation potentials, geometries, relative stabilities, dipole moments, and mean polarizabilities of α- and β-chain P(VDCN-TrCN) models with different TrCN contents. The effects of the chain length and TrCN content on the electrical properties, chain stability, and chain conformation have been examined. Based on the results obtained, the following conclusions can be drawn:

1. The conformational angles are 46° (for *g*) and −80° (for *g′*) in α-chain (*tgtg′*) P$(VDCN\text{-}TrCN)_I$, and 78° (for *g*) and −53° (for *g′*) in P$(VDCN\text{-}TrFE)_{II}$, which should be compared with the angle ±47° in the dimer of the PVDCN homopolymer. The most stable β conformation (*ttt*) for the P(VDCN-TrCN) copolymer is a slightly distorted all-*trans* plane with dihedral angles of 166° for model I and 162° for model II. These angles are very close to the 164° found for the PVDCN homopolymer.
2. The energy differences $E_\beta - E_{\alpha(g)}$ and $E_\beta - E_{\alpha(g')}$ between the β and α conformations are 0.5 and 2.4 kJ mol^{-1} (in model I) and 4.6 and −11.1 kJ mol^{-1} in model II, respectively. All of these values are smaller than the value in PVDCN (5.9 kJ mol^{-1}). This suggests that the stability of the β conformation should be higher in the P(VDCN-TrCN) copolymer than in the PVDCN homopolymer. A situation where the β conformation of P(VDCN-TrCN) is more stable than the α conformation thermodynamically is very useful from the perspective of creating novel materials of interest.
3. The energy barriers for the β→α(*g*) and β→α(*g′*) transitions are 14.5 and 9.5 kJ mol^{-1} in model I and 6.4 and

20.5 kJ mol^{-1} in model II, respectively. The values for model I and the latter value for model II (14.5, 9.5, and 20.5 kJ mol^{-1}) are larger than the barrier (6.9 kJ mol^{-1}) in PVDCN, while the former value for model II (6.4 kJ mol^{-1}) is almost identical to it. Therefore, the β→α transition in P(VDCN-TrCN) should be more difficult to achieve than its equivalent in PVDCN once it is formed. The energy barriers for the α(*g*)→β and α(*g*′)→β transitions are 15.0 and 11.9 kJ mol^{-1} in model I and 11.0 and 25.8 kJ mol^{-1} in model II, respectively. These values are comparable with the values of 11.5 kJ mol^{-1} for PVDCN and 16.3 kJ mol^{-1} for PVDF, except in the case of α(*g*′)→β transitions in model II. This implies that it will be feasible (or slightly more difficult) to prepare a polarized phase of the P(VDCN-TrCN) copolymer.

4. All of the β-chain P(VDCN-TrCN) models with different TrCN contents are curved. The radii of curvature of the β-chain P(VDCN-TrCN) models are slightly larger than the radius of curvature of PVDCN and increase with increasing TrCN content. The alternate copolymer with a mole fraction of TrCN of 0.50 has the largest radius of curvature (about 9.7 Å). Therefore, introducing TrCN into VDCN does not significantly increase the radius of curvature of the copolymer chain. Similar to the PVDCN homopolymer, the bulk P(VDCN-TrCN) copolymer with long chains would be difficult to align in an orderly manner (to enhance its ferroelectricity) and to crystallize. The energy difference per monomer unit, $(E_\beta - E_\alpha)/n$, converges to an almost constant value with increasing chain length, and decreases with increasing TrCN content. The minimum value, about 3.5 kJ mol^{-1}, is seen for P(VDCN-TrCN) with a mole fraction of TrCN of 0.50. This result suggests that P(VDCN-TrCN) will tend to adopt the *trans* conformation, in contrast with the PVDCN homopolymer.
5. For the β-chain P(VDCN-TrCN) models, the dipole moment contribution per monomer unit decreases rapidly with increasing chain length, but increases with increasing TrCN content. For β-chain P(VDCN-TrCN) with 12 monomer units and a mole fraction of TrCN of 0.50, the dipole moment contribution per monomer unit is smaller than those of both β-chain PVDCN with 12 monomer units and β-chain P(VDCN-TrFE) with 12 monomer units. This result suggests that the piezoelectricity of P(VDCN-TrCN) with a mole fraction of TrCN of 0.50 may be comparable with (or slightly smaller than) that of PVDCN, and will be less than that of the P(VDCN-TrFE) copolymer.
6. The mean polarizability per monomer unit of β-chain P(VDCN-TrCN) is slightly higher than that of the α-chain. Chain length does not have a significant effect on the mean polarizability for either α- or β-chain P(VDCN-TrCN). However, its value increases as the TrCN content of P(VDCN-TrCN) increases.

Acknowledgments This work was supported by the Shaanxi Province Education Ministry Research Foundation (11JK0559) and Shaanxi University Technology (SLGQD0709). Some of the calculations were performed at the High Performance Computing Center of Northwestern Polytechnical University.

References

1. Furukawa T (1989) IEEE Trans Electr Insul 24:375–394
2. Lovinger AJ (1983) Science 220:1115–1121
3. Kepler RG, Anderson RA (1992) Adv Phys 41:1–57
4. Eberle G, Schmidt H, Eisenmenger W (1996) IEEE Trans Dielectr Electr Insul 3:624–646
5. Samara GA (2001) Solid State Phys 56:239–458
6. Kawai H (1969) Jpn J Appl Phys 8:975–976
7. Bergman JG Jr, McFee JH, Crane GR (1971) Appl Phys Lett 18:203–205
8. Anderson RA, Kepler RG, Lagasse RR (1981) Ferroelectrics 33:91–94
9. Furukawa T, Date M, Fukada E (1980) J Appl Phys 51:1135–1141
10. Lando JB, Doll WW (1968) J Macromol Sci Phys 2:205–218
11. Farmer BL, Hopfinger AJ, Lando JB (1972) J Appl Phys 43:4293–4303
12. Yagi T, Tatemoto M, Sako JI (1980) Polym J 12:209–223
13. Qu H, Garcia T, Yao W, Zhang J, Ducharme S, Dowben PA, Sorokin AV, Fridkin VM (2003) Appl Phys Lett 82:4322–4324
14. Fukuma T, Kobayashi K, Horiuchi T, Yamada H, Matsushige K (2000) Jpn J Appl Phys Pt 1 39:3830–3833
15. Blinov LM, Fridkin VM, Palto SP, Bune AV, Dowben PA, Ducharme S (2000) Phys Usp 43:243–257
16. Davis GT (1988) In: Wang TT, Herbert JM, Glass AM (eds) Chapter 9. In: The applications of ferroelectric polymers. Bell and Bain, Glasgow, p 37
17. Ducharme S, Palto SP, Fridkin VM, Blinov LM (eds) (2000) Chapter 11. In: Handbook of surfaces and interfaces of materials, vol 3. Academic, San Diego, pp 546–592
18. Wang ZY, Su KH, Fan HQ, Wen ZY (2007) Polymer 48:7145–7155
19. Higashihata Y, Sako J, Yagi T (1981) Ferroelectrics 32:85–92
20. Nakhmanson SM, Buongiorno Nardelli M, Bernholc J (2005) Phys Rev B 72:115210
21. Abe Y, Tashiro K, Kobayashi M (2000) Comput Theor Polym Sci 10:323–333
22. Hattori T, Watanabe T, Akama S, Hikosaka M, Ohigashi H (1997) Polymer 38:3505–3511
23. Hicks JC, Jones TE, Logan JC (1978) J Appl Phys 49:6092–6096
24. Lovinger AJ (1983) Macromolecules 16:1529–1534
25. Wang ZY, Fan HQ, Su KH, Wen ZY (2006) Polymer 47:7988–7996
26. Wang ZY, Fan HQ, Su KH, Wang X, Wen ZY (2007) Polymer 48:3226–3236
27. Lee JW, Ttakase Y, Newman BA, Scheinbeim JI (1991) J Polym Sci Polym Phys 29:273–277
28. Lee JW, Ttakase Y, Newman BA, Scheinbeim JI (1991) J Polym Sci Polym Phys 29:279–286
29. Stupp SI, Carr SH (1979) Colloid Polym Sci 257:913–919
30. Su J, Harrison JS, Clair TS (2000) ISAF 2000: Proc 2000 12th IEEE Int Symp on Appl Ferroelectrics, Honolulu, HI, USA, 21 July–2 Aug 2000, 2:811–814

31. Zheyi M, Scheinbiem JI, Lee JW, Newman BA (1994) J Polym Sci B Polym Phys 32:2721–2731
32. Furukawa T, Goho T, Date M, Takamatsu T, Fukada E (1979) Kobunshi Ronbunshu 36:685–688
33. Pfister G, Abkowitz M, Crystal RG (1973) J Appl Phys 44:2064–2071
34. Tasaka S, Miyasato K, Yoshikawa M, Miyata S, Ko M (1984) Ferroelectrics 57:267–276
35. Petchsuk A (2003) Ferroelectric terpolymers, based on semicrystalline VDF/TrFE/chloro-containing termonomers: synthesis, electrical properties, and functionalization reactions (Ph.D. thesis). The Pennsylvania State University, University Park
36. Tasaka S, Inagaki N, Okutani T, Miyata S (1989) Polymer 30:1639–1642
37. Wang ZY, Su KH, Fan HQ, Wen ZY (2008) Polymer 49:2542–2547
38. Ueda H, Carr SH (1984) Polym J 16:661–667
39. Berlepsch HV, Pinnow M, Stark W (1989) J Phys D Appl Phys 22:1143–1152
40. Ree H, Salomon RE, Labes MM (1979) J Appl Phys 50:3773–3774
41. Furukawa T, Date M, Nakajima K, Kosaka T, Seo I (1988) Jpn J Appl Phys 27:200–204
42. Jo YS, Sakurai M, Inoue Y, Chujo R, Tasaka S, Miyata S (1987) Polymer 28:1583–1588
43. Miyata S, Yoshikawa M, Tasaka S, Ko M (1980) Polym J 12:857–860
44. Jo YS, Inoue Y, Chûjô R, Saito K, Miyata S (1985) Macromolecules 18:1850–1855
45. Tasaka S, Toyama T, Inagaki N (1994) Jpn J Appl Phys 33:5838–5841
46. Gilbert H, Miller FF, Averill SJ, Carlson EJ, Felt VL, Heller HJ, Stewart FD, Sehmidt RF, Trumbull HL (1956) J Am Chem Soc 78:1669–1675
47. Yanko JA, Hawthorne A, Born JW (1958) J Polym Sci 27:145–147
48. Furukawa T, Date M, Nakajima K, Kosaka T, Seo I (1986) Jpn J Appl Phys 25:1178–1182
49. Miyata S, Yoshikawa M, Tasaka S, Ko M (1980) Polym J 12:875–880
50. Jo YS, Maruyama Y, Inoue Y, Chûjô R, Tasaka S, Miyata S (1987) Polym J 19:769
51. Sakurai M, Ohta Y, Inoue Y, Chûjô R (1991) Polym Commun 32:397–399
52. Xiao J, Rosa LG, Poulsen M, Feng DQ, Reddy DS, Takacs JM, Cai L, Zhang J, Ducharme S, Dowben PA (2006) J Phys Condens Matter 18:L155–L161
53. Tajitsu Y, Ogura H, Chiba A, Furukawa T (1987) Jpn J Appl Phys 26:554–560
54. Tasaka S, Miyata S (1985) J Appl Phys 57:906–910
55. Ohigashi H, Omote K, Gomyo T (1995) Appl Phys Lett 66:3281–3283
56. Omote K, Ohigashi H, Koga K (1997) J Appl Phys 81:2760–2769
57. Ounaies Z, Young JA, Harrison JS (1999) Design requirements for amorphous piezoelectric polymers (NASA/CR-2001-211422; ICASE report no. 2001-43). NASA Langley Research Center, Hampton
58. Wang ZY, Su KH, Wang F, Wen ZY (2010) Synth Met 160:2341–2350
59. Wang ZY, Su KH, Jin LX, Wen ZY (2009) Soft Mater 7:296–318
60. Wang ZY, Su KH, Xu Q (2012) J Mater Sci 47:5774–5783
61. Becke AD (1992) J Chem Phys 97:9173–9177
62. Burke K, Perdew JP, Wang Y (1998) In: Dobson JF, Vignale G, Das MP (eds) Electronic density functional theory: recent progress and new directions. Plenum, New York, pp 177–197
63. Frisch MJ, Trucks GW, Schlegel HB et al (2009) Gaussian 09, revision A.02. Gaussian Inc., Wallingford
64. Conciatori AB, Trapasso LE, Stackman RW (1971) In: Mark HF (ed) Encyclopedia of polymer science and technology, vol. 14. Wiley, New York, p 580
65. Solymar L, Walsh D (1988) Lectures on the electric properties of materials, 4th edn. Oxford University Press, Oxford